Centrum voor Wiskunde en Informatica

REPORT*RAPPORT*

MAS

Modelling, Analysis and Simulation

Modelling, Analysis and Simulation

Reduced mixing generates oscillations and chaos in the deep chlorophyll maximum

J. Huisman, N.N. Pham Thi, D.M. Karl, B.P. Sommeijer

REPORT MAS-E0510 JULY 2005

CWI is the National Research Institute for Mathematics and Computer Science. It is sponsored by the Netherlands Organization for Scientific Research (NWO).
CWI is a founding member of ERCIM, the European Research Consortium for Informatics and Mathematics.

CWI's research has a theme-oriented structure and is grouped into four clusters. Listed below are the names of the clusters and in parentheses their acronyms.

Probability, Networks and Algorithms (PNA)

Software Engineering (SEN)

Modelling, Analysis and Simulation (MAS)

Information Systems (INS)

P.O. Box 94079, 1090 GB Amsterdam (NL)
Kruislaan 413, 1098 SJ Amsterdam (NL)
Telephone +31 20 592 9333
Telefax +31 20 592 4199

ISSN 1386-3703

Reduced mixing generates oscillations and chaos in the deep chlorophyll maximum

ABSTRACT
Deep chlorophyll maxima (DCMs) are widespread through large parts of the oceans1-5. These deep layers of high chlorophyll concentration reflect a compromise of phytoplankton growth exposed to two opposing resource gradients: light supplied from above and nutrients supplied from below. It is generally argued that DCMs are stable features. Here we show, however, that reduced vertical mixing can generate oscillations and even chaos in DCMs. These fluctuations in phytoplankton biomass and species composition in the DCM are caused by differences in time scale between two processes: rapid export of sinking phytoplankton withdrawing nutrients from the euphotic zone and the slow upward flux of nutrients fuelling new DCM maxima. Climate models predict that global warming will reduce vertical mixing in the oceans6-9. Our model analysis indicates that this will generate more variability in the phytoplankton dynamics of DCMs, thereby enhancing variability in oceanic primary production and carbon export.

2000 Mathematics Subject Classification: Primary: 65M12, 65M20.
1998 ACM Computing Classification System: G.1.7, G.1.8.
Keywords and Phrases: Advection-diffusion-reaction equations, time integration, stiffness, phytoplankton-nutrient dynamics, oscillation, deep chlorophyll maxima.
Note: Work carried out under subtheme MAS1.1 - Applications from the Life Sciences.

Reduced mixing generates oscillations and chaos in the deep chlorophyll maximum

Jef Huisman[†1], Nga N. Pham Thi[†2], David M. Karl[3] & Ben Sommeijer[2]

[†] *These authors contributed equally to the work.*

[1]*Aquatic Microbiology, Institute for Biodiversity and Ecosystem Dynamics, University of Amsterdam, Nieuwe Achtergracht 127, 1018 WS Amsterdam, The Netherlands.*

[2]*Center for Mathematics and Computer Science (CWI), P.O. Box 94079, 1090 GB Amsterdam, The Netherlands.*

[3]*School of Ocean and Earth Science and Technology, University of Hawaii, 1000 Pope Road, Honolulu, Hawaii 96822, USA*

Deep chlorophyll maxima (DCMs) are widespread through large parts of the oceans[1-5]. These deep layers of high chlorophyll concentration reflect a compromise of phytoplankton growth exposed to two opposing resource gradients: light supplied from above and nutrients supplied from below. It is generally argued that DCMs are stable features. Here we show, however, that reduced vertical mixing can generate oscillations and even chaos in DCMs. These fluctuations in phytoplankton biomass and species composition in the DCM are caused by differences in time scale between two processes: rapid export of sinking phytoplankton withdrawing nutrients from the euphotic zone and the slow upward flux of nutrients fuelling new DCM maxima. Climate models predict that global warming will reduce vertical mixing in the oceans[6-9]. Our model analysis indicates

that this will generate more variability in the phytoplankton dynamics of DCMs, thereby enhancing variability in oceanic primary production and carbon export.

In many waters where the surface mixed layer is depleted of nutrients, subsurface maxima in chlorophyll concentration and phytoplankton biomass are found. Figure 1 shows an example from the North Pacific subtropical gyre, where the deep chlorophyll maximum (DCM) is located at ~100 m depth. DCMs are typically generated by the interplay of several different processes[10-13]. Phytoplankton require both nutrients and light for growth. In oligotrophic oceans, however, the surface layer can be depleted of nutrients by the downward flux of sinking plankton and other organic matter. Nutrients can be replenished by turbulent diffusion of nutrients from below. In waters with limited vertical mixing, these processes favour maximum phytoplankton abundance in the lower euphotic zone, on the edge of nutrient and light limitation. Such DCMs are a permanent feature throughout large regions of the tropical and subtropical oceans[1-4]. Furthermore, seasonal DCMs commonly develop in temperate regions[3,14], and even in the polar oceans[5], when nutrients are depleted in the surface mixed layer with the onset of the summer season.

It is generally believed that DCMs are stable features that track seasonal changes in light and nutrient conditions. However, here we extend recent phytoplankton models[11-13,15,16] to show that the processes leading to the development of a DCM can generate a diffusive instability that may cause oscillations and even chaos in DCMs.

The model is kept as simple as possible, to focus on the key processes involved in the formation of a DCM. We consider a vertical water column of one unit surface area. Let z indicate the depth in the water column, where z runs from 0 at the surface to a maximum depth z_B at the bottom. Let P denote the phytoplankton population density (number of cells/m^3). The population dynamics of the phytoplankton can be described by a reaction-advection-diffusion equation[11-13,15,16]:

$$\frac{\partial P}{\partial t} = growth \; - \; loss - sinking + mixing$$

$$= \mu(N,I)P - mP \; - \; v\frac{\partial P}{\partial z} \; + \; \kappa\frac{\partial^2 P}{\partial z^2} \qquad (1)$$

where $\mu(N,I)$ is the specific growth rate of the phytoplankton as an increasing saturating function of nutrient availability N and light intensity I, m is the specific loss rate of the phytoplankton, v is the phytoplankton sinking velocity, and κ is the vertical turbulent diffusivity. The nutrient dynamics in the water column can be described as[11-13]:

$$\frac{\partial N}{\partial t} = \; -uptake \; + \; recycling + \; mixing$$

$$= -\alpha\mu(N,I)P + \varepsilon\alpha mP + \kappa\frac{\partial^2 N}{\partial z^2} \qquad (2)$$

where α is the nutrient content of the phytoplankton, and ε is the proportion of nutrient in dead phytoplankton that is recycled.

Light intensity, I, is supplied from above and decreases exponentially with depth according to Lambert-Beer's law[15,16]:

$$I = I_{in} \exp\left(-k\int_0^z P(t,\sigma)d\sigma - K_{bg} z \right) \qquad (3)$$

where I_{in} is the incident light intensity, k is the specific light absorption coefficient of the phytoplankton, K_{bg} is the background turbidity of the water column, and σ is an integration variable accounting for the non-uniform phytoplankton population density distribution. To complete the model, we assume zero-flux boundary conditions for the phytoplankton. Furthermore, we assume a zero-flux boundary condition for nutrient at the surface, while nutrient is replenished from below with a fixed concentration N_B at the bottom of the water column. The model is parameterized for clear ocean water, reflecting the example of the North Pacific subtropical gyre (Fig. 1) where the euphotic zone extends to ~100 m depth[4,17].

For extremely high turbulent diffusivities, the model predicts that phytoplankton and nutrients are homogeneously mixed through the water column. In this case, the dynamics of the system are essentially similar to phytoplankton growth in a well-mixed chemostat. For lower turbulent diffusivities, nutrients in the top layer are gradually depleted by sinking plankton. As a result, the nutricline slowly moves downwards, tracked by the phytoplankton population (Fig. 2a). The phytoplankton population slowly declines as the nutrient and light availability diminish, until the population settles at a stable equilibrium at which the downward flux of consumed nutrients equals the upward flux of new nutrients. Thus, a stable DCM develops.

If turbulent diffusivity is reduced even further, however, the DCM no longer settles at a fixed value. Instead, the model predicts that the phytoplankton population in the DCM will oscillate. Depending on the parameter settings the fluctuations in the DCM may range from mild oscillations (Fig. 2b) to pronounced chlorophyll peaks (Fig. 2c). The mechanism that underlies these fluctuations is a diffusive instability. At low diffusivity, the phytoplankton sink relatively fast compared to the slow upward flux of nutrients. As a result, the light conditions of the sinking phytoplankton deteriorate and the phytoplankton population declines. The declining phytoplankton population loses control over the upward nutrient flux, and new nutrients may diffuse further upwards. The upward flux of nutrients reaches a depth where light conditions are suitable for growth. This fuels the next peak in the DCM.

To investigate this phenomenon further, we ran numerous simulations using a wide range of turbulent diffusivities. For comparison, vertical turbulent diffusivities in the ocean interior are typically on the order of 0.1 $cm^2\ s^{-1}$ to 1 $cm^2\ s^{-1}$ (refs. 18,19). The model simulations predict that the DCM becomes unstable when turbulent diffusivity is in the lower end of the realistic range (Fig. 3a). By a cascade of period doublings, reduced turbulent mixing may even generate chaos in the DCM (Fig. 3b).

From a mathematical perspective, the fluctuations in our DCM model resemble diffusive instabilities described for other reaction-diffusion systems[20,21]. Diffusive instabilities in reaction-diffusion systems are often generated by the spatial dispersal of 'resources' and 'consumers' at two different time scales. In our DCM model, the two times scales of spatial dispersal are introduced by the rapid sinking flux of phytoplankton and the slow upward flux of nutrients. Indeed, the period and amplitude of the DCM oscillations increase with increasing phytoplankton sinking velocity (Fig. 3c). Conversely, the period and amplitude decrease with increasing vertical diffusivity (Fig. 3d). Thus, the oscillations become more pronounced if the time scale of sinking is fast compared to the time scale of the upward flux of nutrients.

How would phytoplankton biodiversity respond to fluctuations in the DCM? We developed a multi-species version of our DCM model analogous to earlier phytoplankton competition models[16,22]. An example is shown in Figure 4. Here, the red species is a better light competitor, the blue species is a better nutrient competitor, and the green species is an intermediate competitor for nutrients and light. The simulations show that all three species can coexist in this non-equilibrium environment, which confirms earlier notions that oscillations and chaos promote phytoplankton biodiversity[23]. Furthermore, there is a subtle but consistent vertical zonation, with the highest abundance of the superior nutrient competitor a few meters up in the nutrient-depleted upper zone of the DCM, the peak of the superior light competitor a few meters deeper in the light-deprived lower part of the DCM, and the intermediate competitor squeezed in between. The model predicts that the deep phytoplankton (the red species) oscillates more vehemently than the shallow phytoplankton (the blue species; Fig. 4c-e).

Although simple models can offer only abstractions of real-world phenomena, our model adequately reproduces many features of real-world DCMs. First, the model predicts that the DCM forms at a similar depth of ~100 m and spans a similar depth range as observed in clear oceans waters (compare Fig. 1 and Fig. 2). Second, consistent

with observations, the model predicts that nutrients are depleted to near-zero levels above the DCM while the nutrient concentration increases linearly with depth below the DCM (Fig. 4e; see also ref. 14). Third, detailed studies in the central North Pacific suggest that phytoplankton populations in the DCM indeed show oscillations along a long-term mean[17,24]. Fourth, these detailed DCM studies confirm the prediction of a subtle vertical zonation of species within the DCM, with a phytoplankton community consisting of two main species assemblages whose centres of abundance are vertically separated by several meters in depth[24]. Fifth, as predicted by the model, the deep phytoplankton assemblages in the DCM of the central North Pacific show a larger variability than the shallow phytoplankton assemblages[24]. Further tests of the model predictions will require long-term DCM monitoring programs to establish whether variability in the DCM increases with phytoplankton sinking velocity (Fig. 3c) and reduces with vertical turbulent diffusivity (Fig. 3d).

Climate models predict that global warming will lead to an enhanced stability of the vertical stratification in large parts of the oceans[6,7]. This will reduce vertical mixing and suppress the upward flux of nutrients, leading to a decline in oceanic primary production[7-9]. Our model shows that the same process of reduced vertical mixing may induce oscillations and chaos in the phytoplankton of the DCM, generated by the difference in time scale between the sinking flux of phytoplankton and the upward flux of nutrients. Thus, counter-intuitively, an increased stability of the water column due to global warming may destabilize the phytoplankton dynamics in the DCM, with implications for oceanic primary production, species composition, and carbon export.

Methods

Model simulations. In our simulations, we assume that the specific growth rate of the phytoplankton follows the Monod equation, and is determined by the resource that is most limiting according to Von Liebig's 'law of the minimum'[25]:

$$\mu(N,I) = \mu_{\max} \min\left(\frac{N}{H_N + N}, \frac{I}{H_I + I}\right) \quad (4)$$

where $\mu_{\max}$ is the maximum specific growth rate, H_N and H_I are the half-saturation constants for nutrient-limited and light-limited growth, respectively, and min denotes the minimum function. We note that our results are robust. We found similar results for other formulations of the specific growth rate (e.g., multiplicative functions).

The integral in Eq.3 introduces a nonlocal term in the model. As a result, the model is a system of integro-partial differential equations (integro-PDEs), which is computationally quite demanding. Numerical simulation of the model was based on a finite volume method, with spatial discretisation of the differential operators as well as the integral term. The advection terms were discretised by a third-order upwind biased formula, the diffusion terms by a symmetric second-order formula, and the integral term by the repeated trapezoidal rule[26]. The resulting system of stiff ordinary differential equations was integrated over time using an implicit integration method[27] implemented in the computer code VODE (http://www.netlib.org/ode/). A detailed presentation of our simulation techniques, with tests of the accuracy and numerical stability of the simulations, is presented elsewhere[22,28].

The model was parameterized for clear ocean water[4,29], with realistic turbulent diffusivities[18,19], and growth kinetics typical for nutrient-limited and light-limited phytoplankton[11-13,15,16] (Table 1).

1. Venrick, E. L., McGowan, J.A. & Mantyla, A. W. Deep maxima of photosynthetic chlorophyll in the Pacific Ocean. *Fish. Bull.* **71**, 41-52 (1973).

2. Cullen, J. J. The deep chlorophyll maximum: comparing vertical profiles of chlorophyll *a*. *Can. J. Fish. Aquat. Sci.* **39**, 791-803 (1982).

3. Longhurst, A. R. *Ecological Geography of the Sea* (Academic Press, San Diego, 1998).

4. Letelier, R. M., Karl, D. M., Abbott, M. R. & Bidigare, R. R. Light driven seasonal patterns of chlorophyll and nitrate in the lower euphotic zone of the North Pacific Subtropical Gyre. *Limnol. Oceanogr.* **49**, 508-519 (2004).

5. Holm-Hansen, O. & Hewes, C. D. Deep chlorophyll-*a* maxima (DCMs) in Antarctic waters. I. Relationships between DCMs and the physical, chemical, and optical conditions in the upper water column. *Polar Biology* **27**, 699-710 (2004).

6. Sarmiento, J. L., Hughes, T. M. C., Stouffer, R. J. & Manabe, S. Simulated response of the ocean carbon cycle to anthropogenic climate warming. *Nature* **393**, 245-249 (1998).

7. Bopp, L. *et al*. Potential impact of climate change on marine export production. *Glob. Biogeochem. Cycles* **15**, 81-99 (2001).

8. Sarmiento, J. L. *et al*. Response of ocean ecosystems to climate warming. *Glob. Biogeochem. Cycles* **18**, Art.No.GB3003 (2004).

9. Schmittner, A. Decline of the marine ecosystem caused by a reduction in the Atlantic overturning circulation. *Nature* **434**, 628-633 (2005).

10. Mann, K. H. & Lazier, J. R. N. *Dynamics of Marine Ecosystems* (Blackwell Science, Oxford, 1996).

11. Fennel, K. & Boss, E. Subsurface maxima of phytoplankton and chlorophyll: steady-state solutions from a simple model. *Limnol. Oceanogr.* **48**, 1521-1534 (2003).

12. Hodges, B. A. & Rudnick, D. L. Simple models of steady deep maxima in chlorophyll and biomass. *Deep-Sea Res. I* **51**, 999-1015 (2004).

13. Klausmeier, C. A. & Litchman, E. Algal games: the vertical distribution of phytoplankton in poorly mixed water columns. *Limnol. Oceanogr.* **46**, 1998-2007 (2001).

14. Venrick, E. L. Phytoplankton seasonality in the central North Pacific: the endless summer reconsidered. *Limnol. Oceanogr.* **38**, 1135-1149 (1993).

15. Huisman, J., Arrayás, M., Ebert, U. & Sommeijer, B. How do sinking phytoplankton species manage to persist? *Am. Nat.* **159**, 245-254 (2002).

16. Huisman, J. et al. Changes in turbulent mixing shift competition for light between phytoplankton species. *Ecology* **85**, 2960-2970 (2004).

17. Karl, D. M., Christian, J. R., Dore, J.E., Hebel, D. V., Letelier, R. M., Tupas, L. M. & Winn, C. D. Seasonal and interannual variability in primary production and particle flux at Station ALOHA. *Deep-Sea Research II* **43**, 539-568 (1996).

18. Smyth, W. D., Moum, J. N. & Caldwell, D. R. The efficiency of mixing in turbulent patches: inferences from direct simulations and microstructure observations. *J. Phys. Oceanogr.* **31**, 1969-1992 (2001).

19. Finnigan, T. D., Luther, D. S. & Lukas, R. Observations of enhanced diapycnal mixing near the Hawaiian ridge. *J. Phys. Oceanogr.* **32**, 2988-3002 (2002).

20. Murray, J. D. *Mathematical Biology*, 2nd Ed. (Springer, Berlin, 1993).

21. Okubo, A. & Levin, S. A. *Diffusion and Ecological Problems: Modern Perspectives*, 2nd Ed. (Springer, Berlin, 2001).

22. Huisman, J. & Sommeijer, B. Population dynamics of sinking phytoplankton in light-limited environments: simulation techniques and critical parameters. *J. Sea Res.* **48**, 83-96 (2002).

23. Huisman, J. & Weissing, F. J. Biodiversity of plankton by species oscillations and chaos. *Nature* **402**, 407-410 (1999).

24. Venrick, E. L. Phytoplankton species structure in the central North Pacific, 1973-1996: variability and persistence. *J. Plankton Res.* **21**, 1029-1042 (1999).

25. Von Liebig, J. *Die organische Chemie in ihrer Anwendung auf Agrikultur und Physiologie* (Friedrich Vieweg, Braunschweig, 1840).

26. Hundsdorfer, W. & Verwer, J. G. *Numerical Solution of Time-Dependent Advection-Diffusion-Reaction Equations* (Springer, Berlin, 2003).

27. Brown, P. N., Byrne, G. D. & Hindmarsh, A. C. VODE: a variable-coefficient ODE solver. *SIAM J. Scient. Statist. Comput.* **10**, 1038-1051 (1989).

28. Pham Thi, N. N., Huisman, J. & Sommeijer, B. P. Simulation of three-dimensional phytoplankton dynamics: competition in light-limited environments. *J. Comp. Appl. Math.* **174**, 57-77 (2005).

29. Kirk, J. T. O. *Light and Photosynthesis in Aquatic Ecosystems*, 2nd Ed. (Cambridge Univ. Press, Cambridge, 1994).

Acknowledgements We thank J. Verwer and J. Williams for helpful discussions. The research of J.H. was supported by the Earth and Life Sciences Foundation (ALW), which is subsidised by the Netherlands Organisation for Scientific Research (NWO). N.N.P.T. was supported by the Computational Science program of NWO. D.M.K. acknowledges support from the U.S. National Science Foundation and the Gordon and Betty Moore Foundation. B.S. acknowledges support from the Dutch BSIK/BRICKS project.

Competing interests statement The authors declare that they have no competing financial interests.

Correspondence and requests for materials should be addressed to J.H. (jef.huisman@science.uva.nl).

Table 1 Parameter values and their interpretation

Symbol	Interpretation	Units	Value
Independent variables			
t	time	h	-
z	depth	m	-
Dependent variables			
P	Population density	cells m^{-3}	-
I	Light intensity	µmol photons m^{-2} s^{-1}	-
N	Nutrient concentration	mmol nutrient m^{-3}	-
Parameters			
I_{in}	Incident light intensity	µmol photons m^{-2} s^{-1}	600
K_{bg}	Background turbidity	m^{-1}	0.045
k	Absorption coefficient of phytoplankton	m^2 $cell^{-1}$	6×10^{-10}
z_B	Depth of the water column	m	300
κ	Vertical turbulent diffusivity	cm^2 s^{-1}	0.12
μ_{max}	Maximum specific growth rate	h^{-1}	0.04
H_I	Half-saturation constant of light-limited growth	µmol photons m^{-2} s^{-1}	20
H_N	Half-saturation constant of nutrient-limited growth	mmol nutrient m^{-3}	0.025
m	Specific loss rate	h^{-1}	0.01
α	Nutrient content of phytoplankton	mmol nutrient $cell^{-1}$	1×10^{-9}
ε	Nutrient recycling coefficient	dimensionless	0.5
v	Sinking velocity	m h^{-1}	0.042
N_B	Nutrient concentration at z_B	mmol nutrient m^{-3}	10

Figure 1 Time course of the DCM at Station ALOHA, located in the subtropical Pacific Ocean, North of Hawaii. **a**, Chlorophyll. **b**, Nitrate and nitrite. Data were obtained from the Hawaii Ocean Time-series (HOT) program.

Figure 2 Model simulations at different intensities of vertical mixing. **a**, Stable DCM (κ= 0.50 cm^2/s). **b**, Mild oscillations in the DCM (κ= 0.20 cm^2/s). **c**, Large-amplitude oscillations in the DCM, with a double periodicity (κ= 0.12 cm^2/s). In each subfigure, the left panel shows the phytoplankton dynamics (*P*) while the right panel shows the nutrient dynamics (*N*). Parameter values: see Table 1.

Figure 3 Bifurcation patterns. **a**, Bifurcation diagram showing the local minima and maxima of the oscillating phytoplankton population as a function of turbulent diffusivity. **b**, Detail of the chaotic region in the bifurcation diagram. **c**, The period (blue line) and relative amplitude (red line) of the oscillations increase with phytoplankton sinking velocity. **d**, The period (blue line) and relative amplitude (red line) of the oscillations decrease with vertical turbulent diffusivity. Parameter values: see Table 1.

Figure 4 Competition between 3 phytoplankton species in an oscillating DCM. **a**, Time course of the phytoplankton species. On the long run, the nutrient concentration (**b**) and the phytoplankton species (**c**) settle at a periodic attractor. **d**, Phase plane illustrating the periodic attractor of the phytoplankton species. **e**, Time series of consecutive depth profiles within a single period. Coloured lines: depth profiles of the 3 phytoplankton species; dashed line: light intensity; black line: nutrient concentration. Parameter values as in Table 1, but

with different half-saturation constants for different species. Red species: H_I = 20 µmol photons m^{-2} s^{-1}, H_N = 0.0250 mmol nutrient m^{-3}; green species: H_I = 30 µmol photons m^{-2} s^{-1}, H_N = 0.0190 mmol nutrient m^{-3}; blue species: H_I = 60 µmol photons m^{-2} s^{-1}, H_N = 0.0175 mmol nutrient m^{-3}.

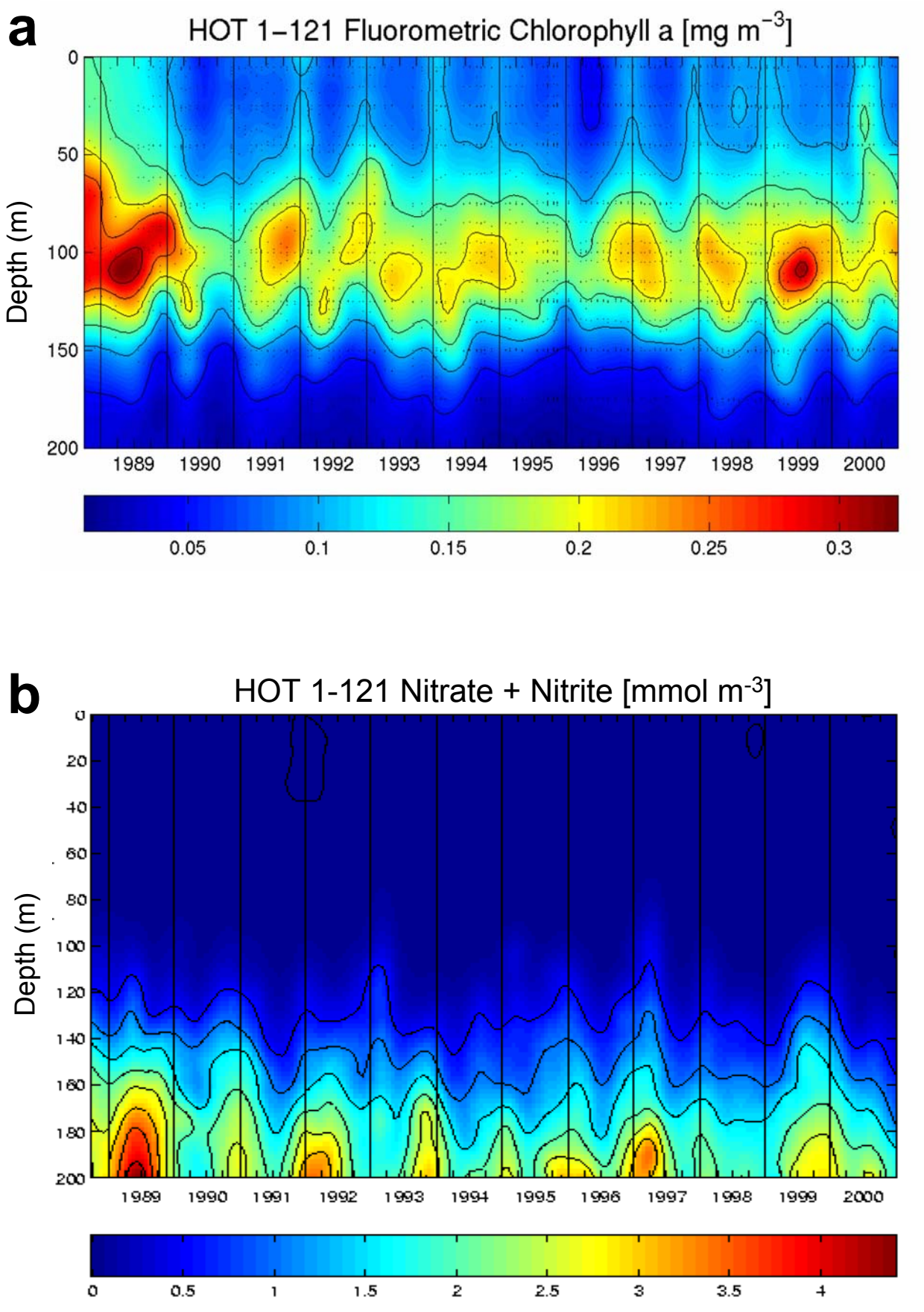
a
HOT 1–121 Fluorometric Chlorophyll a [mg m^{-3}]
Depth (m)
0
50
100
150
200
1989
1990
1991
1992
1993
1994
1995
1996
1997
1998
1999
2000
0.05
0.1
0.15
0.2
0.25
0.3
b
HOT 1-121 Nitrate + Nitrite [mmol m^{-3}]
Depth (m)
0
20
40
60
80
100
120
140
160
180
200
1989
1990
1991
1992
1993
1994
1995
1996
1997
1998
1999
2000
0
0.5
1
1.5
2
2.5
3
3.5
4

Figure 1

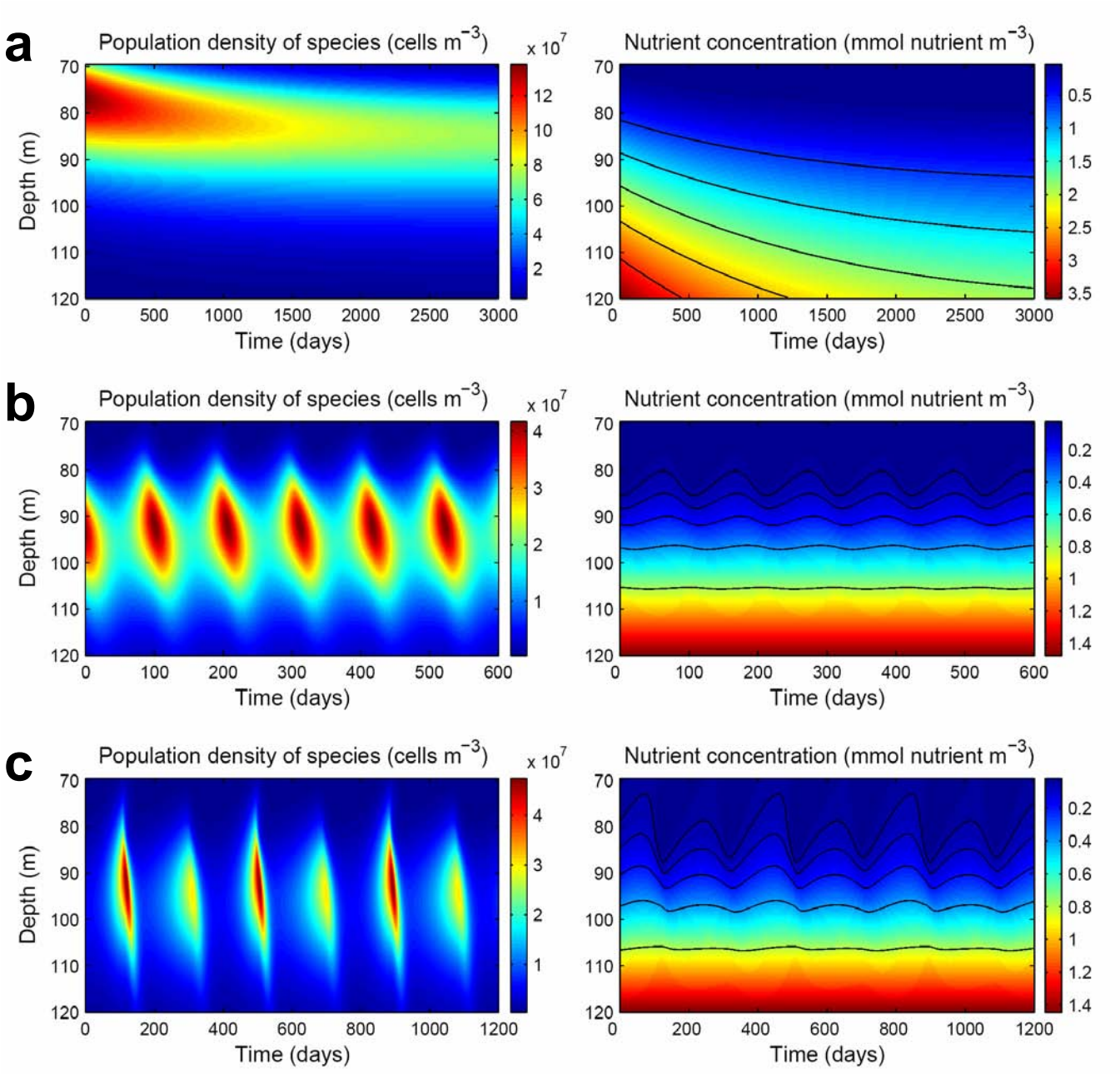
a
Population density of species (cells m^{-3})
x 10^{7}
Depth (m)
Time (days)
Nutrient concentration (mmol nutrient m^{-3})
b
Population density of species (cells m^{-3})
x 10^{7}
Depth (m)
Time (days)
Nutrient concentration (mmol nutrient m^{-3})
c
Population density of species (cells m^{-3})
x 10^{7}
Depth (m)
Time (days)
Nutrient concentration (mmol nutrient m^{-3})

Figure 2

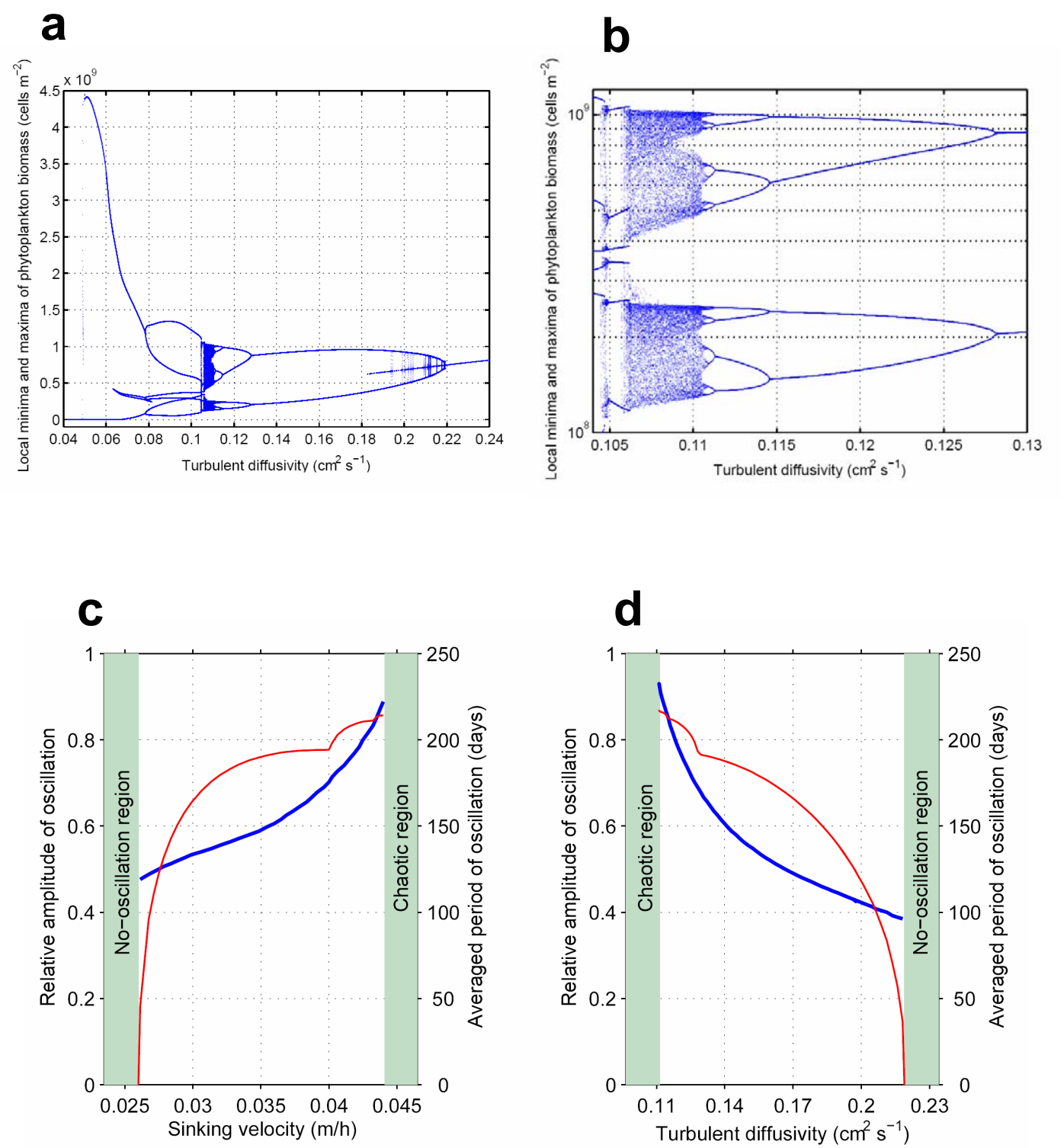
a
x 10^9
Local minima and maxima of phytoplankton biomass (cells m^-2)
Turbulent diffusivity (cm^2 s^-1)
b
Local minima and maxima of phytoplankton biomass (cells m^-2)
Turbulent diffusivity (cm^2 s^-1)
c
Relative amplitude of oscillation
Averaged period of oscillation (days)
No−oscillation region
Chaotic region
Sinking velocity (m/h)
d
Relative amplitude of oscillation
Averaged period of oscillation (days)
Chaotic region
No−oscillation region
Turbulent diffusivity (cm^2 s^-1)

Figure 3

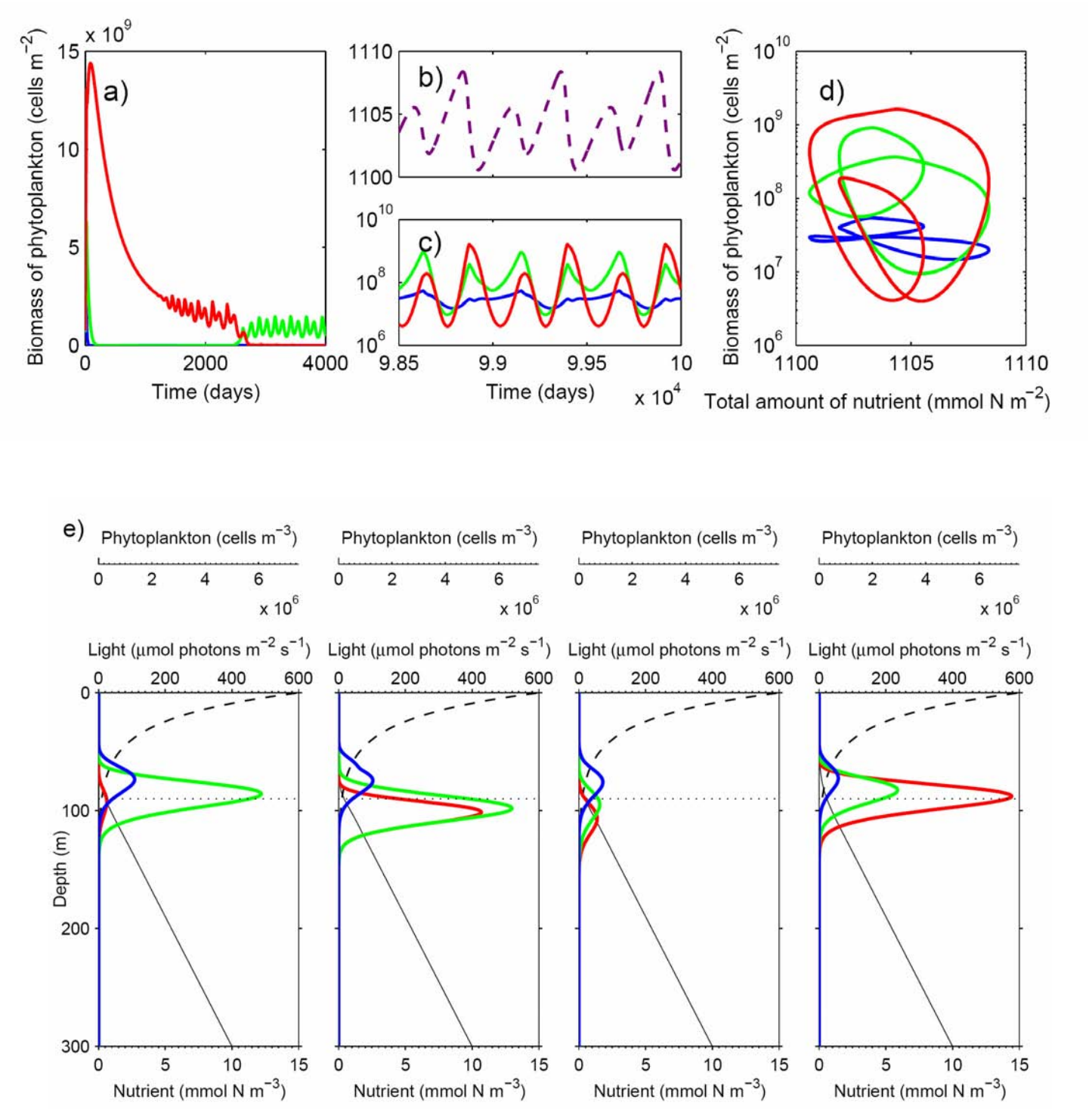
a)
b)
c)
d)
e)
Biomass of phytoplankton (cells m^{-2})
x 10^9
Time (days)
x 10^4
Total amount of nutrient (mmol N m^{-2})
Phytoplankton (cells m^{-3})
x 10^6
Light (µmol photons m^{-2} s^{-1})
Depth (m)
Nutrient (mmol N m^{-3})

Figure 4